Earthquake Engineering, Tenth World Conference © 1992 Balkema, Rotterdam. ISBN 90 5410 060 5

High frequency response of a sediment-filled valley for seismic waves

Shinozaki Yuzo
Kyoto University, Japan

ABSTRACT: Time-domain responses as well as frequency-domain responses of a sediment-filled valley for incident SH waves are studied with the emphasis of site responses for high frequencies ($> 1\ Hz$) which are of interest in earthquake engineering. Calculating them using a boundary integral equation method , we discuss in details effects of inclined interfaces of the valley upon wave amplification patterns , propagation of Love waves and duration of the ground shaking in the valley.

1 INTRODUCTION

It has been recognized that the dynamic behavior of a structure during an earthquake is considerably affected by the geologic formation and the dynamic property of the soil medium. In particular, the topographic irregularities in the soil medium seem to have tremendous effects on the characteristics of earthquake ground motion, together with associated structural damages of buildings. Though there have been many theoretical studies about the elastic wave propagation in or around such geologic and topographic irregularities of the soil medium(e.g., Aki, 1988), few studies about its effects for high frequencies have been performed. Therefore, in this study time-domain responses as well as frequency-domain responses of a sediment-filled valley for incident plane SH waves are investigated with emphasis of site responses for high frequencies ($> 1\ Hz$). Assuming two main types of geometrical structures referred to as type 1 (cosine-shape) and type 2 (U-shape) valleys (Bard and Bouchon, 1980), we have calculated them using a boundary integral equation method.

2 METHOD OF ANALYSIS

Geometry of the problem is shown in Figure 1. A sediment-filled valley is assumed to be a two-dimensional model (denoted by medium I) , which is characterized by mass density, ρ_1, and shear wave velocity, β_1. Medium I is surrounded by a half-space medium (denoted by medium II), which is characterized by mass density, ρ_2 , and shear wave velocity, β_2. An interface between the media I and II is denoted by Γ_2 and perfect bonding along the interface is understood. The material of them is assumed to be linearly elastic, homogeneous and isotropic. The interface is defined in the same way as Bard and Bouchon(1980). In all the models studied here, the width of the valley, $2D$, is assumed to be equal to $10km$, and d_2/h is assumed to be equal to 5.0 for type 2 valley. Three shape ratios are studied h/D : 0.02, 0.04, and 0.06 (i.e., $h = 100m$, $200m$, and $300m$).

The problem is of the anti-plane strain type, i.e., both the media I and II extend to infinity perpendicular to the plane of the drawing and the motion of them takes place along y axis only. Two different curves are defined inside and outside the interface Γ_2 along which single layer potentials are assumed for the analysis by the so-called indirect boundary integral equation method.

Let us denote the displacements of the soil deposit (medium I) and the surrounding half-space (medium II) for SH-type motion, by u_1 and u_2 , each of which satisfies the scalar Helmholtz's equation in its domain of definition.

$$\frac{\partial^2 u_j}{\partial x^2} + \frac{\partial^2 u_j}{\partial y^2} + \kappa_j^2 u_j = 0, \quad (j = 1,\ 2), \tag{1}$$

where $\kappa_j = \omega/\beta_j$, $(j = 1,\ 2)$ is the wavenumber, and β_1 and β_2 are the shear wave velocities in the media I and II, respectively. Throughout the analysis, the time factor $exp(i\omega t)$ is understood.

The scattered wave field is expressed in terms of single layer potentials as follows:

$$u_1(\mathbf{r}) = \int_{c_2} \sigma_2(\mathbf{r}_0) \mathrm{G}_1(\mathbf{r}, \mathbf{r}_0) \mathrm{dS}_0 \tag{2a}$$

$$u_2(\mathbf{r}) = \int_{c_1} \sigma_1(\mathbf{r}_0) \mathrm{G}_2(\mathbf{r}, \mathbf{r}_0) \mathrm{dS}_0 + u^{inc}(\mathbf{r}), \tag{2b}$$

with an incident wave of

$$u^{inc}(\mathbf{r}) = e^{-i\omega(x\ sin\theta_0/\beta_2 - z\ cos\theta_0/\beta_2)}, \tag{2c}$$

where $\mathbf{r} = (x\ ,\ z)$ and $\mathbf{r}_0 = (x_0,\ z_0)$ are the position vectors for the "observation" and "source" points, respectively, and c_2 is the surface defined in the half-space outside of the interface Γ_2 and c_1 is the surface defined inside of the interface Γ_2. The functions $\mathrm{G}_1(\mathbf{r}, \mathbf{r}_0)$ and $\mathrm{G}_2(\mathbf{r}, \mathbf{r}_0)$ are the Green's functions for the half-space in the media I and II, respectively. The density functions $\sigma_1(\mathbf{r}_0)$ and $\sigma_2(\mathbf{r}_0)$ are yet to be determined. θ_0 is an angle of incidence of SH wave.

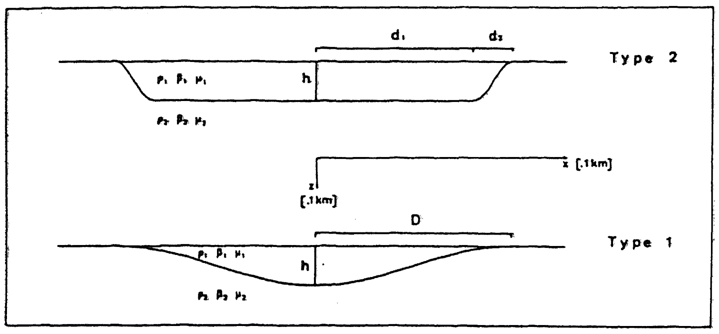

Figure 1. Geological configuration of valley studied. ρ, β, and μ represent respectively for each medium, its density, shear wave velocity, and rigidity (after Bard and Bouchon:1980). Density and shear wave velocity in each medium are assumed to be $\rho_1 = 2.0\ ton/m^3,\ \beta_1 = 0.5km/sec$, and $\rho_2 = 2.3\ ton/m^3,\ \beta_2 = 1.3km/sec$, respectively.

The Green's functions are given by (Lamb,1904)

$$G_1(\mathbf{r},\mathbf{r}_0) = \frac{1}{4i\pi\mu_1}\int_{-\infty}^{\infty}\frac{e^{-ik(x-x_0)}}{\gamma_1}\cdot(e^{-i\gamma_1|z-z_0|} + e^{-i\gamma_1(z+z_0)})dk \quad (3a)$$

$$G_2(\mathbf{r},\mathbf{r}_0) = \frac{1}{4i\pi\mu_2}\int_{-\infty}^{\infty}\frac{e^{-ik(x-x_0)}}{\gamma_2}\cdot e^{-i\gamma_2|z-z_0|}dk, \quad (3b)$$

where

$$\gamma_j = ((\omega/\beta_j)^2 - k^2)^{1/2},\ Im(\gamma_j) \leq 0, \quad (j = 1, 2).$$

The boundary condition of zero stress at the free surface of the medium is already satisfied through deriving equations (2). There are still two remaining boundary conditions, necessary for determining the total of two density functions, $\sigma_1(\mathbf{r}_0)$ and $\sigma_2(\mathbf{r}_0)$; they are given by

$$u_1(\mathbf{r}) = u_2(\mathbf{r}), \qquad \mathbf{r}\ on\ \Gamma_2 \quad (4a)$$

$$\mu_1\frac{\partial u_1(\mathbf{r})}{\partial \mathbf{n}} = \mu_2\frac{\partial u_2(\mathbf{r})}{\partial \mathbf{n}}, \qquad \mathbf{r}\ on\ \Gamma_2 \quad (4b)$$

where μ_1 and μ_2 are the shear moduli of the media I and II, respectively.

Imposing the boundary conditions upon equations (2), we get the following boundary integral equations associated with two unknown density functions $\sigma_1(\mathbf{r}_0)$ and $\sigma_2(\mathbf{r}_0)$.

$$\int_{c_2}\sigma_2(\mathbf{r}_0)G_1(\mathbf{r},\mathbf{r}_0)dS_0 = \int_{c_1}\sigma_1(\mathbf{r}_0)G_2(\mathbf{r},\mathbf{r}_0)dS_0 + u^{inc}(\mathbf{r}),\ \mathbf{r}\ on\ \Gamma_2 \quad (5a)$$

$$\left(\frac{\mu_1}{\mu_2}\right)\int_{c_2}\sigma_2(\mathbf{r}_0)\frac{\partial G_1(\mathbf{r},\mathbf{r}_0)}{\partial \mathbf{n}}dS_0 = \int_{c_1}\sigma_1(\mathbf{r}_0)\frac{\partial G_2(\mathbf{r},\mathbf{r}_0)}{\partial \mathbf{n}}dS_0 + \frac{\partial u^{inc}(\mathbf{r})}{\partial \mathbf{n}},\ \mathbf{r}\ on\ \Gamma_2. \quad (5b)$$

In order to solve this boundary integral equations, a discretization scheme is introduced. Let's assume that the density functions represent a system of discrete line sources along c_1 and c_2 , i.e.,

$$\sigma_1(\mathbf{r}_0) = \sum_{m=1}^{M} a_m\delta(|\,\mathbf{r}_0 - \mathbf{r}_m\,|),\quad \mathbf{r}_m\ on\ c_1 \quad (6a)$$

$$\sigma_2(\mathbf{r}_0) = \sum_{n=1}^{N} b_n\delta(|\,\mathbf{r}_0 - \mathbf{r}_n\,|),\quad \mathbf{r}_n\ on\ c_2, \quad (6b)$$

where δ denotes the Dirac's delta function. Then equations (5) can be written as follows:

$$\sum_{m=1}^{M} a_m G_2(\mathbf{r}_k,\mathbf{r}_m) - \sum_{n=1}^{N} b_n G_1(\mathbf{r}_k,\mathbf{r}_n) = -u^{inc}(\mathbf{r}_k)$$

$$\mathbf{r}_k\ on\ \Gamma_2,\quad k = 1, 2, \cdots, K \quad (7a)$$

$$\sum_{m=1}^{M} a_m\frac{\partial G_2(\mathbf{r}_k,\mathbf{r}_m)}{\partial \mathbf{n}_k} - \left(\frac{\mu_1}{\mu_2}\right)\sum_{n=1}^{N} b_n\frac{\partial G_1(\mathbf{r}_k,\mathbf{r}_n)}{\partial \mathbf{n}_k} = -\frac{\partial u^{inc}(\mathbf{r}_k)}{\partial \mathbf{n}_k}$$

$$\mathbf{r}_k\ on\ \Gamma_2,\quad k = 1, 2, \cdots, K. \quad (7b)$$

Equations (7) can be rewritten in an abbreviated form by

$$\mathbf{AX} = \mathbf{G}, \quad (8)$$

where $\mathbf{A}$ is a $(2K) \times (M + N)$ matrix. When a value of $(2K)$ is chosen to be equal to that of $(M + N)$, a density vector $\mathbf{X}$ can be determined uniquely. But the matrix $\mathbf{A}$ tends to become ill-conditioned . In order to prevent to become ill-conditioned, a value for $(2K)$ is chosen larger than that for $(M + N)$, and the least square method is applied to solve. This can lead to solve the following equations:

$$\mathbf{X} = (\mathbf{A}^*\mathbf{A})^{-1}\mathbf{A}^*\mathbf{G} \quad (9)$$

where superscript * indicated in $\mathbf{A}^*$ denotes the transposed conjugate matrix of the coefficient matrix $\mathbf{A}$.

Once the coefficient a_m and b_n are solved numerically from equation (9) , the displacement field on the ground can be calculated by the following equations.

$$u_1(\mathbf{r}) = \sum_{n=1}^{N} b_n G_1(\mathbf{r},\mathbf{r}_n) \quad (10a)$$

$$u_2(\mathbf{r}) = \sum_{m=1}^{M} a_m G_2(\mathbf{r},\mathbf{r}_m) + u^{inc}(\mathbf{r}). \quad (10b)$$

It is seen from the above mentioned procedures that it takes a large percentage of time to calculate the Green's functions in equations (7) and their derivatives. As we cannot evaluate analytically the Green's functions, we usually have to carry out a formidable task to compute a lot of numerical integrations of infinite integrals whose integrands show a rapid oscillation when the position of receiver $\mathbf{r}$ is far from that of source $\mathbf{r}_0$. Following the method proposed by Campillo and Bouchon(1985), we assume that the medium configuration is periodic in the x-direction with a spatial periodicity L so as to use discrete wavenumber Green's functions efficiently. They are expressed by

$$G_{1n}(\mathbf{r},\mathbf{r}_0) = \frac{1}{2i\pi L\mu_1}\sum_{n=-\infty}^{n=\infty}\frac{e^{-ik_n(x-x_0)}}{\gamma_{1n}}\cdot\left(e^{-i\gamma_{1n}|z-z_0|} + e^{-i\gamma_{1n}(z+z_0)}\right) \qquad (11a)$$

$$G_{2n}(\mathbf{r},\mathbf{r}_0) = \frac{1}{2i\pi L\mu_2}\sum_{n=-\infty}^{n=\infty}\frac{e^{-ik_n(x-x_0)}}{\gamma_{2n}}\cdot e^{-i\gamma_{2n}|z-z_0|} \qquad (11b)$$

with

$$k_n = n\frac{2\pi}{L}$$

$$\gamma_{jn} = ((\omega/\beta_j)^2 - k_n^2)^{1/2}, \quad Im(\gamma_{jn}) \le 0, \qquad (j = 1, 2).$$

To introduce the effect of attenuation, the real S wave velocities β_j are replaced by complex ones (Horike et al., 1990) according to the rule

$$\frac{1}{\beta_j} \Rightarrow \frac{1}{\beta_j}\left(1 - \frac{i}{2Q_j}\right),$$

where Q_j are the quality factors of S waves.

3 NUMERICAL RESULTS

Figures 2 show amplitude characteristics of frequency-domain responses of type 1 as well as type 2 valley due to vertically propagating plane SH waves.

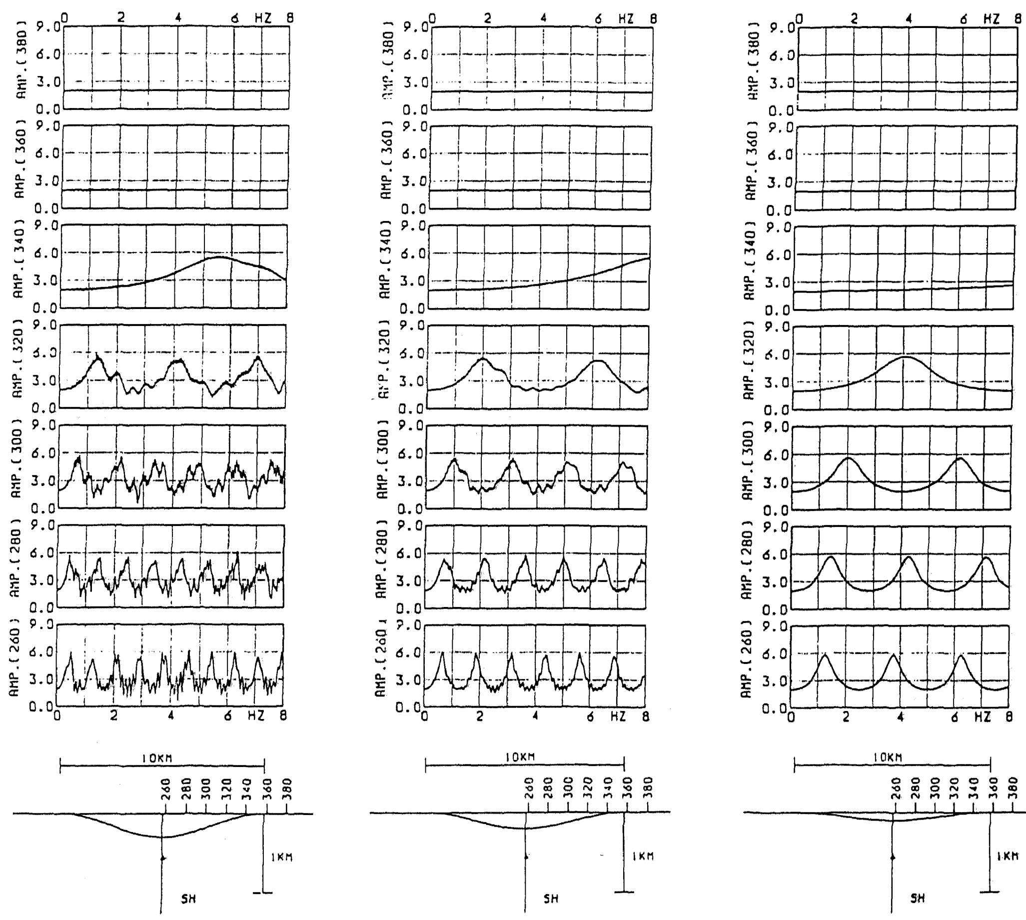

Figure 2a. Frequency responses of type 1 valley with maximum depth h = 300m, 200m and 100m, half-width D = 5 km and quality factors $Q_1 = Q_2 = 10000$ due to vertically propagating SH waves. Periodicity length L = 25.6 Km.

The normalized amplitude characteristics of seven sites indicated by 260 through 380 are calculated up to 8 Hz. Seven sites are selected at every 1 Km distant. Since the impedance contrast between the upper layer and the lower medium is assumed to be a comparatively high value, it is expected that the effect of the valley on responses of the harder surrounding medium should be small and that the normalized responses of every site located at outside of the valley should remain to be the constant value, i.e., 2 , over the whole interval of frequency.

Three sites near central part of type 2 valley, i.e., 260 , 280 and 300, show predominant peaks in the vicinity of the resonant frequencies while the valley consists of a flat layer. Some responses of type 2 valley also show rapid oscillating ripples, but those responses of type 1 valley do not show such oscillating ripples because the inclined interfaces of type 1 valley are less steep than those of type 2 valley. Since the effect of the interface on the site response increases according as the site approaches to the edge of the valley, their responses tend to show different trends from those of the central sites. It is noted that site 340 just above the inclined interface shows a broad-band peaks different from those of another sites.

Figures 3 show time-domain responses of seven sites of type 2 valley due to an artificial earthquake ground input motion, indicated by "INPUT", which has a predominant frequency at about 4 Hz. Those responses except two sites, 360 and 380 outside of the valley, clearly show propagation of Love waves generated from both inclined interfaces of the valley. An example of time-domain response of a flat layer which has the same impedance contrast and layer depth as type 2 valley due to the same excitation as the former case is also shown on the top of the figure. Its wave form does not depend upon the site and since no Love waves propagates, its duration of ground shaking lasts just as long as that of incident ground motion. Some spectral ratios of surface ground motion within the valley to that of site 380 are

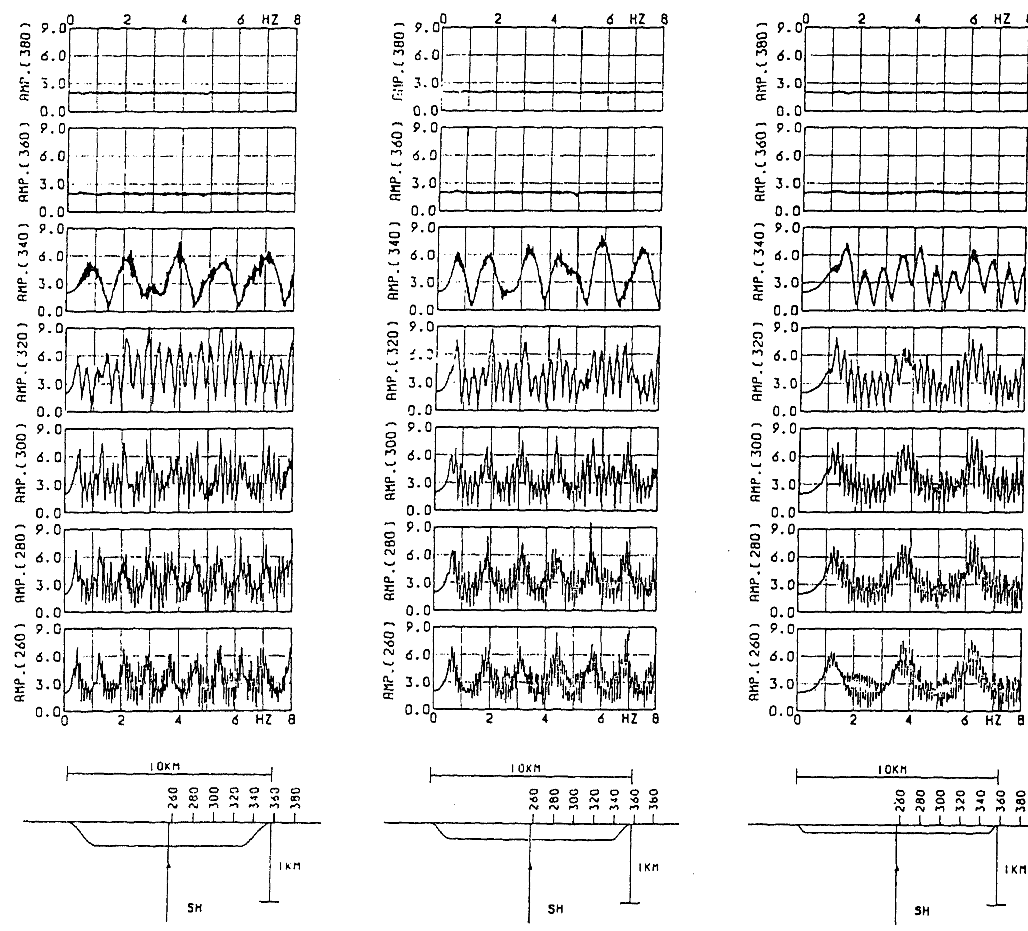

Figure 2b. Frequency responses of type 2 valley with maximum depth h = 300m, 200m and 100m, half-width D = 5 km and quality factors Q_1 = Q_2 = 10000 due to vertically propagating SH waves. Periodicity length L = 25.6 Km.

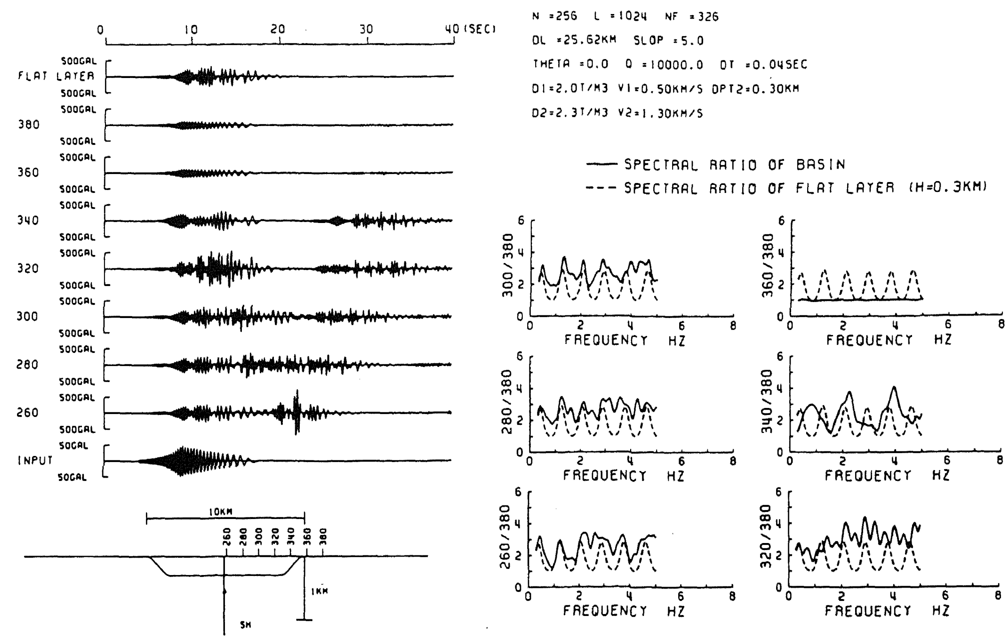

Figure 3a. Time-domain responses and spectral ratios of surface ground motion of type 2 valley to bed rock motion with maximum depth h = 300m, half-width D = 5 km and quality factors $Q_1 = Q_2 = 10000$ due to a vertically propagating earthquake ground motion which has a predominant frequency at about 4 Hz.

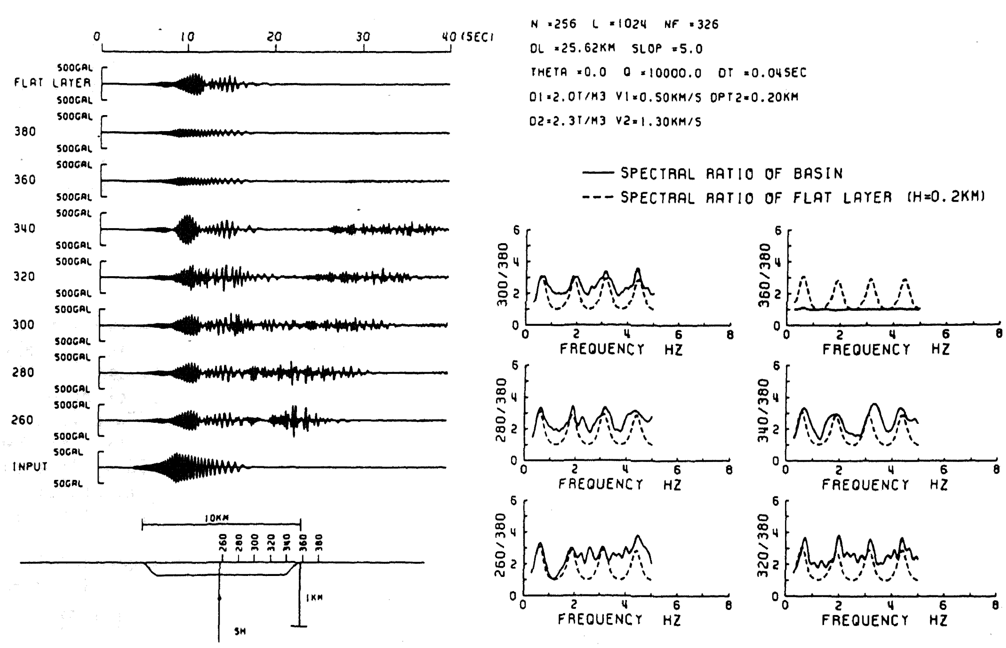

Figure 3b. Time-domain responses and spectral ratios of surface ground motion of type 2 valley to bed rock motion with maximum depth h = 200m, half-width D = 5 km and quality factors $Q_1 = Q_2 = 10000$ due to a vertically propagating earthquake ground motion which has a predominant frequency at about 4 Hz.

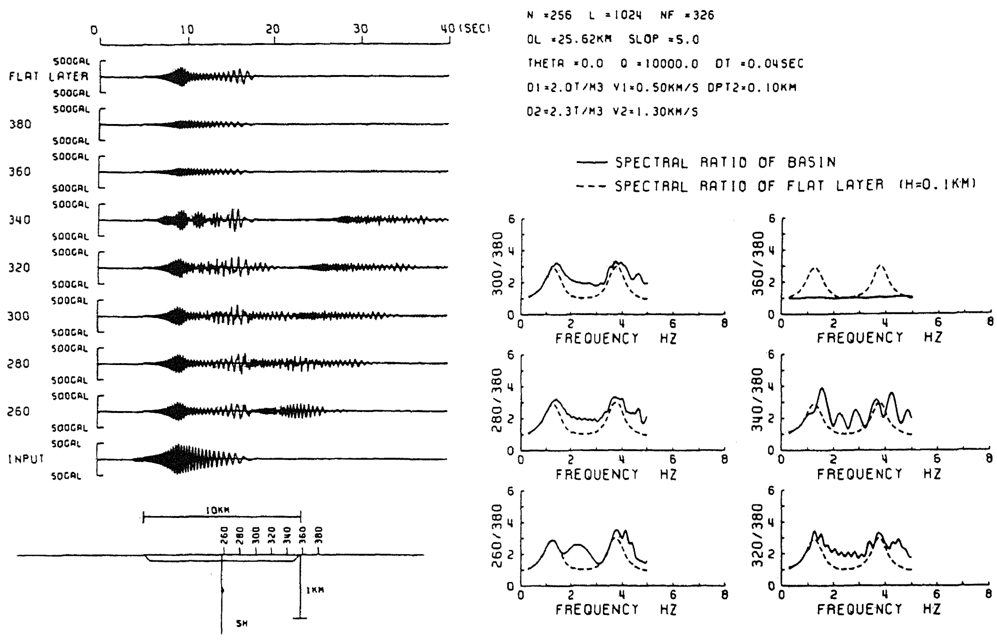

Figure 3c. Time-domain responses and spectral ratios of surface ground motion of type 2 valley to bed rock motion with maximum depth h = 100m, half-width D = 5 km and quality factors $Q_1 = Q_2 = 10000$ due to a vertically propagating earthquake ground motion which has a predominant frequency at about 4 Hz.

also calculated based on the acceleration responses at several sites due to the earthquake ground motion. They are indicated by solid line curves. We also show spectral ratio of the flat layer response to the response of site 380 indicated by broken line curve in this figure. Spectral ratio of the flat layer response simply shows amplification at the resonant frequencies. However, since Love waves generated from both inclined interfaces seem to have a great influence on the wave form and duration of responses of type 2 valley as shown in time-domain responses, spectral ratios of 5 sites within the valley show more complicated amplification than the flat layer response and they become more broad-band than that of the flat layer response.

4 CONCLUDING REMARKS

Time-domain responses as well as frequency-domain responses of a sediment-filled valley for incident SH waves are studied with the emphasis of site responses for high frequencies (> 1 Hz). We calculate them using a boundary integral equation method in which Green's functions are evaluated using the discrete wavenumber method.

Frequency-domain responses of surface ground motion show that predominant frequencies of surface ground motion decrease with increase of the depth as well as S wave velocity of surface layer and that surface ground motion is amplified as much as surface ground motion of the flat layer response. Some spectral ratios of surface ground motion to bedrock motion are also calculated based on the acceleration responses at several sites due to an artificial earthquake ground input motion which has relatively high predominant frequencies and they are compared with spectral ratios of the flat layer response to bedrock motion. It is shown that since Love waves generated by the inclined interface have a great influence on the responses of the valley, spectral ratios of sediment-filled valley become more broad-band than that of the flat layer response.

REFERENCES

Aki, K.(1988). Local site effects on strong ground motion, Recent advances in ground-motion evaluation, ASCE Geotechnical Special Publication 20, 103-155.

Bard, P. Y. and M. Bouchon(1980). Seismic response of sediment-filled valleys Part 1: The case of incident SH waves, *Bull. Seism. Soc. Am.*, 70, 1263-1286.

Campillo, M. and M. Bouchon(1985). Synthetic SH seismograms in a laterally varying medium by discrete wavenumber method, *Geophys. J. R. Astr. Soc.*, 83, 307-317.

Horike, M., H. Uebayashi, and Y. Takeuchi(1990). Seismic response in three-dimensional sedimentary basin due to plane S wave incidence, *J. Phys. Earth*, 38, 261-284.

Lamb, H.(1904). On the propagation of tremors over the surface of elastic solid, *Phil. Trans. Royal Soc. London*, A, 203, 1-42.